Experimental results for a pressure reducer control with a modular actuator

Yassine Ariba, Frédéric Gouaisbaut, Flavien Deschaux, François Roux, François Dugué

Experimental results for a pressure reducer control with a modular actuator*

Yassine Ariba[1], Frédéric Gouaisbaut[2], Flavien Deschaux[3], François Roux[4] and François Dugué[4]

***Abstract*— This paper addresses the control of a pressure regulator which reduces the pressure from an upstream chamber to a desired lower pressure in a downstream one. Most results in the literature, either neglect the actuator dynamic embedded in the reducer, or develop a specific design dedicated to their system. In this study, we propose to take into account this inner dynamic with a control system designed independently. The objective is to enable a modular architecture. It also justifies classical cascade control approach. A modeling work of the physical system combined with some practical assumptions provides a simple linear model. An output feedback control is designed to ensure stability, performance requirements and to cope with a saturation nonlinearity. This phenomenon is necessarily present due to physical limitations of the fluid flow rate in the actuator. Robust analysis approach and sector condition are used to address this feature as well as to take into account the dynamic of the independent controlled actuator with reduced assumptions on this subsystem. Stability condition of the overall system is expressed with LMI tests. Simulation and experimental tests show the validity of the proposed methodology.**

I. INTRODUCTION

Pressure regulation is an essential aspect of many industrial and technical processes. It involves controlling the pressure of a fluid or gas within a system to ensure optimal performance and safety. Pressure regulation is used in a wide range of applications, from medical systems [14], water supply networks [2], drilling mechanism [13] to chemical processing and automotive engine [5], [12], [1], [6]. In this context, many control laws have been developed in an ad hoc way, often taking into account the characteristics of the overall pressure system in order to maintain the stability of the operating point despite pressure calls from external environment. Various methods can be found, as the simplest control laws such as PI or PID, which are effective for linearized models around the operating points [7], [12], as well as more advanced control laws such as LQR, sliding mode [8], [6], backstepping [14] or switched control laws [13]. These control laws allow to take into account some nonlinearities that are common to many pressure control systems, such as saturation of the inlet flow valve or to make the closed loop system robust to external disturbances. However, in many works [2], the dynamic of the servo motor that drives the valve, and thus the flow, are not taken into account. In general, the assumption is reasonable if we consider that this dynamic is much faster than the dynamic of pressure regulation. Otherwise, the inner dynamic can have an important impact and may reduce the performance of the global controlled system.

In this paper, we are interested in the design of a control law for an experimental pressure reducing device. The application context concerns an actuator for pressure control on a launcher. These regulators are used to expand helium from tanks at 400 bar to lower pressures (from a few bars to a few tens of bar) depending on the equipment requirements. They are in particular in charge of the pressurization of the propellant tank and thus ensure the injection in the combustion chamber (see Figure 1 for a simplistic principle scheme). For instance, such mechanism is used in the propulsion system of the Aestus engine at the storable propellant stage (EPS) of Ariane 5. Currently, the regulators are mechanical/pneumatic technologies and are passive. The development of an innovative electronic regulator[1], which will be digitally controlled, with an adapted control system, will make it possible to maintain a constant downstream pressure despite disturbances (flow calls, temperature, vibrations). This technology also has the advantage of being flexible in use since the pressure set point can be modified digitally and during operation, unlike conventional regulators which are fixed manually for a specific setting and for the entire duration of the mission [11].

The proposed control law is designed independently of the actuator dynamics. However, the study of the stability of the operating point is carried out by taking into account the dynamics of a generic actuator, admitting a limited number of assumptions, especially the existence of a Lyapunov function for the set point of the actuator. Finally, the proposed methodology is illustrated on simulations and an experiment on a test bench is conducted to compare results and to validate the methodology.

II. SYSTEM MODELING

A. Description of the reducer

A principle schematic of the pressure reducer with the actuator is given in Figure 2. As illustrated, in our work and testbed, an electromagnetic actuator is used to control the valve position. Nevertheless, this study aims at designing a control law for the pressure reducer independently of

*This work was partly supported by the company CSTM and the CNES, the french national space agency.

[1]Y. Ariba is with the laboratory LAAS-CNRS, Université de Toulouse, INSA, Toulouse, France yariba@laas.fr

[2]F. Gouaisbaut is the laboratory LAAS-CNRS, Université de Toulouse, UPS, Toulouse, France fgouaisb@laas.fr

[3]F. Deschaux is with the company Comat, 31130 Flourens, France f.deschaux@comat.space

[4]F. Roux and F. Dugué are with the company CSTM, 31320 Castanet-Tolosan, France contact@cstm.fr

[1]Patents: FR3007855 (2015) and FR3121193 / WO2022200710 (2023).

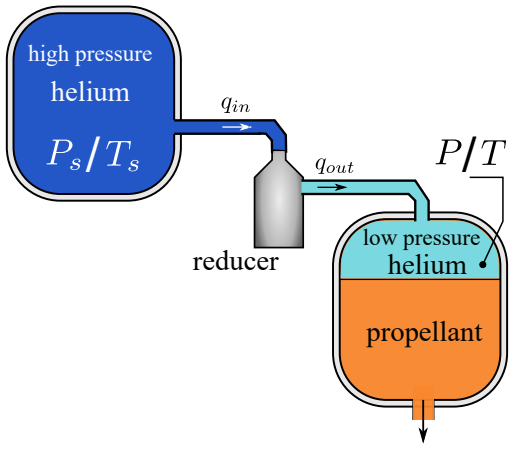

Fig. 1. *Launcher application.*

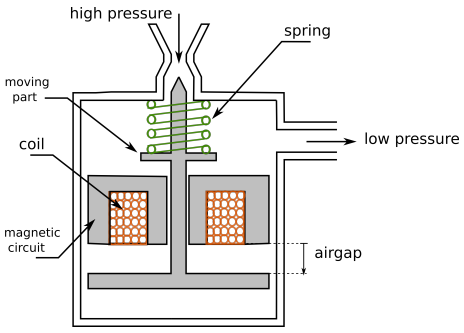

Fig. 2. *Principle schematic of the pressure reducer / actuator.*

the technology of the positioning system. This objective is to allow a modular architecture which is interesting for reusability of equipment and to simplify the control design (as in cascade control approach). We intend then to prove the overall stability property with reduced knowledge on the controlled actuator / servomotor. From a control point of view, the structure of the system is depicted in Figure 3. Basically, the positioning actuator controls the position of a moving mechanical part, which itself changes the fluid flow rate (a gas in our application), modifying the opening of the flow cross section, from a upstream chamber to a downstream one.

B. Modeling

Applying thermodynamical laws, an analytical model is proposed for the pressure dynamic. To this end a set of general assumptions are made, and particularly relevant for the launcher application.

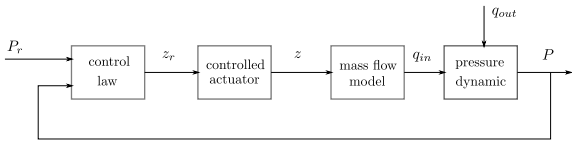

Fig. 3. *Block diagram of the feedback control system.*

Assumption 1:

(a) In the studied application, we always have $P_s/P > 2$, hence sonic flow is considered.
(b) The ideal gas law can be applied.
(c) The gas expansion and compression are adiabatic transformations. It implies there is no heat transfer between the system and its environment.
(d) The temperature of the gas downstream of the actuator is constant. Experiments on our setup have shown that the temperature decreased very slightly and this phenomenon can be neglected.

By Assumption 1b, let us invoke the ideal gas law, we have at the downstream side of the actuator:

$$PV = nRT$$

where all variables and parameters are defined in Table I and depicted in Figure 1. Introducing the mass of the gas $m = nM$ and its specific gas constant $R_{spec} = R/M$, the law is rewritten as

$$PV = mR_{spec}T.$$

Differentiating the above equation,

$$V\frac{dP}{dt} = R_{spec}T\frac{dm}{dt},$$

and considering that the mass variation $\dot{m}$ can be modeled by the difference of the mass flow rate $q_{in} - q_{out}$, a dynamic model for the pressure is obtained:

$$\dot{P} = k\Big(q_{in} - q_{out}\Big) \tag{1}$$

with $k = \frac{R_{spec}T}{V}$. This latter is constant by Assumption 1d. This modeling approach allows us to derive a simple integrator model. Experimentation will show that this model is sufficient, though an accurate value for parameter k is required, to capture the pressure dynamic of our testbed.

The inlet flow is controlled by a positioning actuator that modifies the cross-sectional area at the bottleneck S_{in}. Because the flow is sonic (Assumption 1a), the mass flow rate does not depend on the downstream pressure P and is modeled by

$$q_{in} = \rho_{in}S_{in}C_{in} \tag{2}$$

with ρ_{in} the mass density and C_{in} the fluid velocity at the bottleneck. These two parameters can be determined by the equations of an adiabatic process (Assumption 1c). In that case, the flow velocity can be expressed as

$$C_{in} = \sqrt{\gamma\frac{P_{in}}{\rho_{in}}} = \sqrt{\gamma R_{spec}T_{in}}$$

where γ is the Laplace constant, P_{in} and T_{in} are, respectively the pressure and the temperature at the bottleneck. The second inequality derives from the ideal gas law and noticing that $R_{spec} = \frac{nR}{\rho_{in}V_{in}}$. Then, the temperature at the bottleneck T_{in} can be expressed in relation to the upstream temperature

T_s from the adiabatic process equations, $T_{in} = \frac{2T_s}{\gamma+1}$. T_s being considered as constant, so is the flow velocity,

$$C_{in} = \sqrt{2\gamma R_{spec}\frac{T_s}{\gamma+1}}. \tag{3}$$

Regarding the mass density at the bottleneck, it can be expressed, still from the adiabatic process equations, in relation to the upstream mass density ρ_s as

$$\rho_{in} = \rho_s \left(\frac{T_{in}}{T_s}\right)^{\frac{1}{\gamma-1}} = \rho_s \left(\frac{2}{\gamma+1}\right)^{\frac{1}{\gamma-1}} \tag{4}$$

The second equality stems from the above-mentioned expression of T_{in}. At last, the opening area is a static function of the needle position $S_{in}(z)$. This function is defined by the mechanical design of the valve needle and the seat. In practice, analytical calculation to establish the relationship between z and S_{in} is very complicated because of the complex neck shape designed from fluid mechanics requirements. Numerical simulations have been therefore conducted with a mechanical engineering Computer-Aided Design software (see Figure 5) to measure the cross-sectional area for different positions of the needle. A polynomial approximation provides a satisfactory model, as shown in Figure 4. Note that with this approach, for different neck geometry the following methodology is still valid and the design development remains unchanged. Then, combining (3) and (4), the mass flow rate (2) equals

$$q_{in} = \rho_s \left(\frac{2}{\gamma+1}\right)^{\frac{1}{\gamma-1}} S_{in}(z)\sqrt{2\gamma R_{spec}\frac{T_s}{\gamma+1}}$$

Upstream parameters ρ_s and T_s being considered as constant over the duration of an experiment, all coefficients can be lumped with the polynomial coefficients of $S_{in}(z)$. Finally, one obtain a model for the mass flow block in Figure 3, a static function of the form:

$$q_{in} = f_{bn}(z) = c_2 z^2 + c_1 z + c_0 \tag{5}$$

with c_i being known constant parameters that mainly depend on the design of the bottleneck and the supply tank state. However, the opening area is necessarily limited and it thus saturates the flow. Let us define $sat_1(\cdot)$ an asymmetric saturation function such that

$$sat_1(q_{in}) = \begin{cases} q_{\min} & \text{if} \quad q_{in} < q_{\min} \\ q_{in} & \text{if} \quad q_{\min} < q_{in} < q_{\max} \\ q_{\max} & \text{if} \quad q_{in} > q_{\max} \end{cases} \tag{6}$$

Assumption 2: The static function f_{bn} modeling the relationship between the needle position and the mass flow is assumed to be a monotonically increasing function. Furthermore, regarding the inverse function, it is also assumed that there exist α, a known positive scalar such that:

$$\frac{\left|f_{bn}^{-1}(x_2) - f_{bn}^{-1}(x_1)\right|}{\left|x_2 - x_1\right|} \leq \alpha$$

Symbols	Description	Units
P_s	Supply pressure (high)	Pa
P	Downstream pressure (to be regulated)	Pa
T_s	Temperature in the supply tank	K
T	Temperature in the downstream chamber	K
V	Volume of the downstream chamber	m^3
q_{in}	Inlet flow rate	g/s
q_{out}	Oulet flow rate	g/s
m	Mass of the gas	g
M	Molar mass	g mol^{-1}
n	Amount of substance	mol
R	Ideal gas constant	J mol^{-1} K^{-1}
R_{spec}	Specific gas constant = R/M	J K^{-1} g^{-1}

TABLE I

NOMENCLATURE FOR KEY VARIABLES/PARAMETERS.

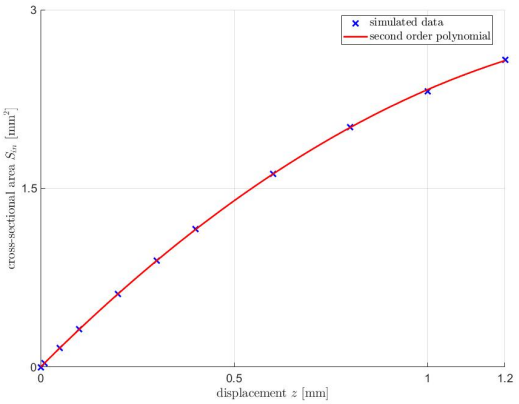

Fig. 4. *Opening area at the bottleneck w.r.t. the needle position of the actuator.*

III. CONTROL LAW DESIGN

A. Control law design without the actuator dynamics

At this stage, we consider the design of a control law without taking into account the actuator controlling the position of the valve. In that case, the pressure dynamic is modeled by equation (1) with q_{in} being the (virtual) control input. The key idea is to simplify the control design by decoupling subsystems, and to lead to a modular approach. Let us add an extra state variable, as the integral of the difference between the setpoint and the measure, to include an integral effect in the control law to reject constant disturbances and ensure a zero static error. Then, we define a state space model as

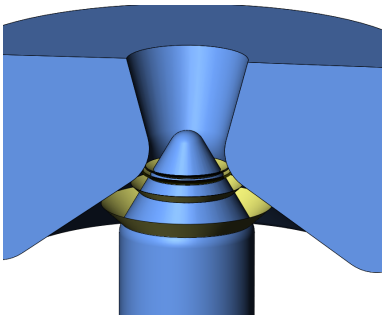

Fig. 5. *Computer-Aided Design model for the valve opening.*

follows, with $x_1 = P$ and $x_2 = \int_0^t P(\theta) - P_{ref}\, d\theta$,

$$\begin{cases} \dot{x}_1 = & k\Big(sat_1(q_{in}) - q_{out}\Big) \\ \dot{x}_2 = & x_1 - P_{ref} \end{cases}$$

When the actuator dynamic is neglected, the inlet flow q_{in} can be considered as the control signal. Applying a state feedback control of the form $q_{in} = k_1(x_1 - P_{ref}) + k_2 x_2$, the unique equilibrium point is $x_{eq} = [P_{ref} \quad q_{out}/k_2]^T$. Defining the error state vector $e = x - x_{eq}$, the closed-loop error dynamic is described by

$$\begin{cases} \dot{e}_1 = & k\Big(sat_1(k_1 e_1 + k_2 e_2 + q_{out}) - q_{out}\Big) \\ \dot{e}_2 = & e_1 \end{cases} \tag{7}$$

Note that, the region of linearity for the above system is defined by the set

$$\mathcal{R}_L = \Big\{ e \in \mathbb{R}^2 \mid \underbrace{q_{\min} - q_{out}}_{<0} \leq k_1 e_1 + k_2 e_2 \leq \underbrace{q_{\max} - q_{out}}_{>0} \Big\}$$

For $e \in \mathcal{R}_L$, system (7) with error coordinates is merely a second order linear system and state feedback gains k_1 and k_2 can easily be designed to ensure local stability around the origin as well as desired performance requirements. We aim at taking into account the saturation phenomenon and better estimate the region of stability of the setpoint equilibrium. Indeed, experimental tests have shown that, upon pressure setpoint changes, the valve generally hits its limits as such the saturation can not be ignored.

Inspired from [9], let define the dead-zone function $\phi(\theta) = sat_1(\theta + q_{out}) - \theta - q_{out}$ so as to reformulate system (7) into

$$\dot{e} = \underbrace{\begin{bmatrix} kk_1 & kk_2 \\ 1 & 0 \end{bmatrix}}_{A} e + \underbrace{\begin{bmatrix} k \\ 0 \end{bmatrix}}_{B} \phi(Ke) \quad \text{with } K = \begin{bmatrix} k_1 & k_2 \end{bmatrix} \tag{8}$$

Function ϕ is depicted in Figure 6. Note that it is asymmetric w.r.t. the ordinate axis and the dead-zone range depends on the outflow rate q_{out}. Even though, this latter can be seen as a disturbance for the pressure control, its presence is necessary to include the origin in the linear mode of system (8).

At this stage, the generalized sector condition can be applied to cope with the nonlinear term in (8). Let define the set

$$S(K - G, q_{\min} - q_{out}, q_{\max} - q_{out}) = \Big\{ e \in \mathbb{R}^2 \mid q_{\min} - q_{out} \leq (K - G)e \leq q_{\max} - q_{out} \Big\}$$

where matrix $G \in \mathbb{R}^{1\times 2}$ is a free matrix that will define the sector, and thus the region of attraction to be estimated. The corresponding sector condition is

$$\phi(Ke)^T M \Big(\phi(Ke) + Ge\Big) \leq 0$$

with M any positive scalar. An example of sector is illustrated in Figure 6 for the particular choice $G = \lambda K$, with $0 < \lambda < 1$. Then, from the above condition a theorem for the local asymptotic stability of (8) can be stated.

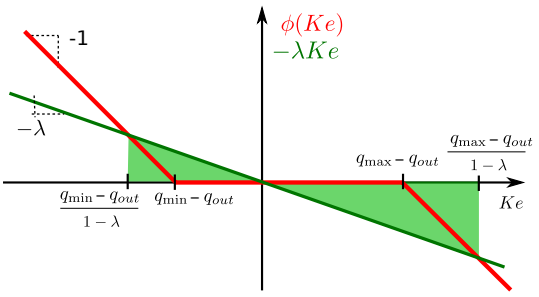

Fig. 6. *Dead-zone function ϕ and sector model.*

Theorem 1: For given gains k_1 and k_2 such that matrix A in (8) is Hurwitz. If there exist a matrix $Z \in \mathbb{R}^{1\times 2}$, a scalar $U > 0$ and a positive definite matrix $W \in \mathbb{R}^{2\times 2}$ such that

$$\begin{pmatrix} WA^T + AW & BU - Z^T \\ UB^T - Z & -2U \end{pmatrix} < 0$$

and

$$\begin{pmatrix} W & WK^T - Z^T \\ KW - Z & u_0^2 \end{pmatrix} \geq 0$$

where $u_0^2 = \min\Big\{(q_{\min} - q_{out})^2, (q_{\max} - q_{out})^2\Big\}$, then the origin for the system (8) is locally asymptotically stable (LAS). The region of attraction is estimated by the ellipsoid

$$\varepsilon(X, 1) = \Big\{ e \in \mathbb{R}^2 \mid e^T X e \leq 1 \Big\} \qquad \text{with} \quad X = W^{-1}$$

Proof: The proof is similar to [10], [9] and only a sketch is proposed. The proof is based on the use of a quadratic Lyapunov function $V(e) = e^T X e$. The first LMI is derived from the definite negativeness condition for the Lyapunov function derivative along the trajectories of (8), while the second one defines the ellipsoid that is included in the polyhedral set $S(K - G, q_{\min} - q_{out}, q_{\max} - q_{out})$. The decision variables Z and U correspond, respectively, to GW and M^{-1}. Differently from [9], we have adapted the definition of parameter μ_0 to cope with the asymmetric feature of the saturation. ■

B. Taking into account the actuator dynamics

Most results in the literature, either neglect the actuator dynamic that controls the valve opening, or develop a specific design dedicated to their setup. Such actuators may be autonomous systems that are controlled independently from the usage. In this paper, a modular approach is proposed where the control laws of the actuator and the pressure reducer are designed separately. Then, the overall stability must be analyzed. We intend to propose a general methodology that can be readily adapted for different applications with some assumptions.

The actuator used in our pressure regulator is an electromagnetic actuator that drives the valve with a linear motion. In previous work, a backstepping control law has been designed to ensure an asymptotically stable and accurate positioning system [4]. Generally speaking, the closed-loop model for the controlled actuator could be of the form

$$\begin{cases} \dot{\eta} = f_a(\eta, z_r) \\ \delta z = C_a \eta \end{cases} \tag{9}$$

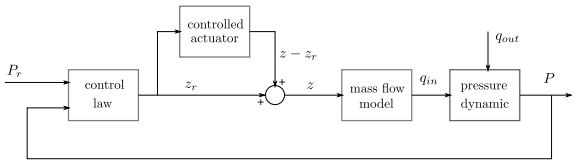

Fig. 7. *Block diagram of the feedback control system emphasizing the position deviation δz.*

where the state η corresponds to the error coordinates of the actuator state variables (typically, the valve position, the velocity and the coil current) w.r.t. the equilibrium point and the reference signal z_r. Its dynamic is nonlinear in general. Only the output $\delta z = z - z_r$ is assumed to be linear in the state η. It is thus considered that a previous study has designed a control law that ensures the asymptotic stability of (9) and the convergence of z toward z_r.

Assumption 3: It is assumed that the origin of system (9) is the unique equilibrium point, $\forall z_r \in \mathbb{R}$, and is asymptotically stable. Thus, z converges toward the desired reference z_r. It is also assumed that a Lyapunov function $V_a(\eta)$ for the aforementioned system is known and is such that $\dot{V}_a(\eta) \leq -\eta^T Q_a \eta$, with $Q_a \in \mathbb{R}^{n_a \times n_a}$ a positive definite matrix.

Let redraw the block diagram in Figure 3 into the one in Figure 7 to emphasize the impact of the deviation of the actual actuator position from the ideal one. This latter correspond to the control law as designed in the previous section

$$z_r = f_{bn}^{-1}\big(Ke + q_{out}\big)$$

where $f_{bn}^{-1}(\cdot)$ is the reciprocal function of $f_{bn}(\cdot)$ in (5). Consequently, the potential inlet flow rate is now expressed as:

$$\begin{aligned} q_{in} =& f_{bn}\Big(z_r + \delta z\Big) = f_{bn}\Big(f_{bn}^{-1}\Big(Ke + q_{out}\Big) + \delta z\Big) \\ =& f_{bn}\Big(f_{bn}^{-1}\Big(Ke + q_{out}\Big)\Big) + c_2\delta z^2 \\ &+ 2c_2\delta z \underbrace{f_{bn}^{-1}\Big(Ke + q_{out}\Big)}_{z_r} + c_1\delta z \\ =& Ke + q_{out} + \delta z \underbrace{\Big(c_2\delta z + 2c_2 z_r + c_1\Big)}_{\Delta} \end{aligned}$$

In that case, the error system (7) is expressed as

$$\begin{cases} \dot{e}_1 = & k\Big(sat_1(Ke + q_{out} + \delta z\Delta) - q_{out}\Big) \\ \dot{e}_2 = & e_1 \end{cases} \tag{10}$$

Clearly, when the position deviation δz is set to 0 (considering the closed-loop dynamic of the actuator as perfect), the model of the previous section is recovered. Note that the equilibrium point x_{eq} for $x-$coordinate, and thus 0 for $e-$coordinate, has not changed since $\delta z = 0$ at the equilibrium by Assumption 3. The new region of linearity for the above system is now defined by

$$\mathcal{R}_L = \Big\{e \in \mathbb{R}^2 \mid q_{\min} - q_{out} \leq Ke + \delta z\Delta \leq q_{\max} - q_{out}\Big\}$$

Let us model Δ as a bounded uncertain parameter and define the augmented state ξ and gain $\bar{K}$:

$$\Delta \in [\Delta_1\ ,\ \Delta_2] \quad \xi = \begin{bmatrix}\eta \\ e\end{bmatrix} \quad \text{and} \quad \bar{K} = \begin{bmatrix}\Delta C_a & K\end{bmatrix}$$

The same dead-zone function $\phi(\theta)$ is proposed but with a different argument $\theta = Ke + \delta z\Delta = \bar{K}\xi$. Combining (9) and (10), the whole pressure reducing system, including the valve control dynamic, can be expressed as

$$\begin{cases} \dot{\eta} = f_a(\eta, z_r) \\ \dot{e} = \underbrace{\begin{bmatrix} kk_1 & kk_2 \\ 1 & 0 \end{bmatrix}}_{A} e + \underbrace{\begin{bmatrix} k\Delta C_a \\ 0 \end{bmatrix}}_{B_1} \eta + \underbrace{\begin{bmatrix} k \\ 0 \end{bmatrix}}_{B} \phi(\bar{K}\xi) \end{cases} \tag{11}$$

In order to deal with the nonlinear deadzone function, let redefine the set

$$\begin{aligned} &S(\bar{K} - G, q_{\min} - q_{out}, q_{\max} - q_{out}) = \\ &\quad \Big\{\xi \in \mathbb{R}^{n_a+2} \mid q_{\min} - q_{out} \leq (\bar{K} - G)\xi \leq q_{\max} - q_{out}\Big\} \end{aligned}$$

where matrix $G \in \mathbf{R}^{1 \times n_a+2}$ is a free matrix that defines the generalized sector condition

$$\phi(\bar{K}\xi)^T M\Big(\phi(\bar{K}\xi) + G\xi\Big) \leq 0 \tag{12}$$

with M any positive scalar. The following theorem proposes a stability condition for the pressure regulator when the actuator dynamic, for which the control system has been designed independently, is now taken into account.

Theorem 2: Under Assumptions 2 and 3, for given gains k_1 and k_2 such that matrix A in (11) is Hurwitz, if there exist matrices $Z \in \mathbb{R}^{1\times 2}$ and $G_1 \in \mathbb{R}^{1 \times n_a}$, a scalar $U > 0$ and a positive definite matrix $W \in \mathbb{R}^{2\times 2}$ such that

$$\begin{bmatrix} -Q_a & B_1(\Delta_i)^T & -G_1^T \\ B_1(\Delta_i) & WA^T + AW & BU - Z^T \\ -G_1 & UB^T - Z & -2U \end{bmatrix} < 0 \tag{13}$$

for $i = \{1, 2\}$ and

$$\begin{pmatrix} W & WK^T - Z \\ (WK^T - Z)^T & u_0^2 \end{pmatrix} \geq 0 \tag{14}$$

where $u_0^2 = \min\Big\{(q_{\min} - q_{out})^2, (q_{\max} - q_{out})^2\Big\}$, then the origin for the system (11) is locally asymptotically stable (LAS).

Proof: Consider the Lyapunov function candidate

$$V(\xi) = V_a(\eta) + e^T X e$$

with $X \in \mathbb{R}^{2\times 2}$ a positive definite matrix and V_a a Lyapunov function introduced in Assumption 3 and associated to the controlled actuator. Let us calculate its time-derivative:

$$\begin{aligned} \dot{V}(\xi) =& \ \dot{V}_a(\eta) + 2e^T X\dot{e} \\ &\leq -\eta^T Q_a \eta + 2e^T XAe + 2e^T XB_1\eta + 2e^T XB\phi(\bar{K}\xi) \end{aligned}$$

$\forall \xi \in S(\bar{K}-G, q_{\min}-q_{out}, q_{\max}-q_{out})$, we have

$$\begin{aligned}\dot{V}(\xi) \leq & -\eta^T Q_a \eta + 2e^T XAe + 2e^T XB_1\eta \\ & + 2e^T XB\phi(\bar{K}\xi) - 2\phi(\bar{K}\xi)^T M\Big(\phi(\bar{K}\xi)+G\xi\Big) \\ \leq & \begin{bmatrix}\eta\\ e\\ \phi(\bar{K}\xi)\end{bmatrix}^T \Xi(\Delta) \begin{bmatrix}\eta\\ e\\ \phi(\bar{K}\xi)\end{bmatrix}\end{aligned}$$

with

$$\Xi(\Delta) = \begin{bmatrix} -Q_a & B_1(\Delta)^T X & -G_1^T M \\ XB_1(\Delta) & A^T X + XA & XB - G_2^T M \\ -MG_1 & B^T X - MG_2 & -2M \end{bmatrix}$$

and $G = [G_1\ G_2]$. This first inequality stems from Assumption 3 and the second one introduces the sector condition (12). Hence, proving $\Xi(\Delta) < 0$, $\forall \Delta \in [\Delta_1\ ,\ \Delta_2]$, implies that $\dot{V}(\xi)$ is negative definite. Matrix $\Xi(\Delta)$ being linear in Δ, it is sufficient to test the condition on its bound as in polytopic approach. Consequently, if the two conditions: $\Xi(\Delta_1) < 0$ and $\Xi(\Delta_2) < 0$ are satisfied, then $\dot{V}(\xi) < 0$ $\forall \xi \in S(\bar{K}-G, q_{\min}-q_{out}, q_{\max}-q_{out})\setminus\{0\}$ and $\dot{V}(0) = 0$. In that case, function V is thus a Lyapunov function for system (11) and the LAS of the origin is proven. By left and right multiplying both $\Xi(\Delta_i)$ by $\text{diag}(\mathbb{I}_{n_a}, X^{-1}, M^{-1})$ and denoting $U = M^{-1}$, $X^{-1} = W$ and $Z = G_2 W$, the conditions are LMI, which can be tested efficiently. ■

In a second step, the second LMI (14) in Theorem 2 defines an ellipsoidal set for e

$$\varepsilon(X,1) = \{e \in \mathbb{R}^2 \mid e^T X e \leq 1\} \quad \text{with } X = W^{-1}$$

that is included in the polyhedral $S(\bar{K} - G, q_{\min} - q_{out}, q_{\max} - q_{out})$. The limit of this ellipsoidal set corresponds to a level curve for the projection of the Lyapunov function $V(\xi)$ on the e plane. It could thus provide an estimation of the basin of attraction w.r.t. state variable e. However, the uncertain parameter

$$\Delta = c_2\delta z + 2c_2 z_r + c_1 = c_2\delta z + 2c_2 f_{bn}^{-1}(Ke + q_{out}) + c_1$$

depends on e and η, and was assumed to be bounded. It is required to make sure to select Δ_1 and Δ_2 such that for all $e \in \varepsilon$, it implies that $\Delta \in [\Delta_1\ ,\ \Delta_2]$. So that the uncertain modeling does not affect the region of attraction. The conditions are stated in the following proposition.

Proposition 1: For a given nominal q_{out} and for a given maximal deviation $\bar{\delta z}$, if Theorem 2 and the two inequalities

$$\Delta_1 \leq 2c_2 f_{bn}^{-1}(q_{out}) + c_1 - |c_2\bar{\delta z}| - 2\alpha|c_2|\ \|K\|\frac{1}{\sqrt{\lambda_{\min}(X)}}$$

$$\Delta_2 \geq 2c_2 f_{bn}^{-1}(q_{out}) + c_1 + |c_2\bar{\delta z}| + 2\alpha|c_2|\ \|K\|\frac{1}{\sqrt{\lambda_{\min}(X)}}$$

are satisfied, then an estimation of the basin of attraction is given by the ellipsoidal set

$$\varepsilon(X,1) = \{e \in \mathbb{R}^2 \mid e^T X e \leq 1\} \quad \text{with } X = W^{-1} \quad (15)$$

where W is obtained from the resolution of the aforementioned LMI (14).

Proof: First, let us redefine the uncertainty Δ. When the whole system is at the equilibrium: $e = 0$ and $z = z_r \Rightarrow \delta z = 0$. In that case, the uncertainty equals $\Delta_0 = 2c_2 f_{bn}^{-1}(q_{out}) + c_1$. A new expression is

$$\Delta = \Delta_0 + \delta_\Delta$$

where

$$\delta_\Delta = \Delta - \Delta_0 = c_2\delta z + 2c_2\Big(f_{bn}^{-1}(Ke + q_{out}) - f_{bn}^{-1}(q_{out})\Big)$$

Using Assumption 2, this latter quantity can be bounded by

$$|\delta_\Delta| \leq |c_2\delta z| + |2c_2\alpha Ke| \leq |c_2\delta z| + 2\alpha|c_2|\ \|K\|\|e\|$$

In addition, for all $e \in \varepsilon(X,1)$ (15), we have

$$\|e\|^2 \leq \frac{1}{\lambda_{\min}(X)}$$

Assuming a maximal position deviation $\bar{\delta z}$,

$$|\delta_\Delta| \leq |c_2\bar{\delta z}| + 2\alpha|c_2|\ \|K\|\frac{1}{\sqrt{\lambda_{\min}(X)}}$$

Hence, choosing the uncertain range of δ_Δ with

$$\Delta_1 \leq \Delta_0 - |c_2\bar{\delta z}| - 2\alpha|c_2|\ \|K\|\frac{1}{\sqrt{\lambda_{\min}(X)}}$$

$$\Delta_2 \geq \Delta_0 + |c_2\bar{\delta z}| + 2\alpha|c_2|\ \|K\|\frac{1}{\sqrt{\lambda_{\min}(X)}}$$

we ensure that when $e \in \varepsilon(X,1)$, it implies that $\Delta \in [\Delta_1\ ,\ \Delta_2]$. The conservative modeling with the uncertain parameter Δ does not restrain the estimation of the region of attraction. ■

The next step is to validate the proposed theory through simulations and experimentation.

IV. Simulation and experimental results

This section presents the simulation results with MATLAB/Simulink software and the experimental results performed on our testbed. Numerical values for system parameters are not given for confidentiality reasons.

A. Simulations

Considering the augmented system (8), consisting of the physical model and an integral action, the state feedback gain K has been designed with the classical pole placement method to ensure A is hurwitz and have the dead-zone free system converging in approximately 2 seconds. Then, Theorem 2 is applied to prove that the whole system, with the nonlinearities (flow rate saturation + static function f_{bn}) and taking into account the actuator dynamic (with a control law designed beforehand independently), is locally asymptotically stable and that the pressure P converges to the reference P_{ref}. Let us consider a linear servomotor, asymptotically stable and for which the derivative of the Lyapunov function is bounded by a quadratic form with $Q_a = 300\mathbb{I}_3$ (see Assumption 3). Regarding Assumption 2, the CAD model provides numerical values for the bottleneck function f_{bn} (5), see Figure 4, and the bound α was computed $\alpha =$

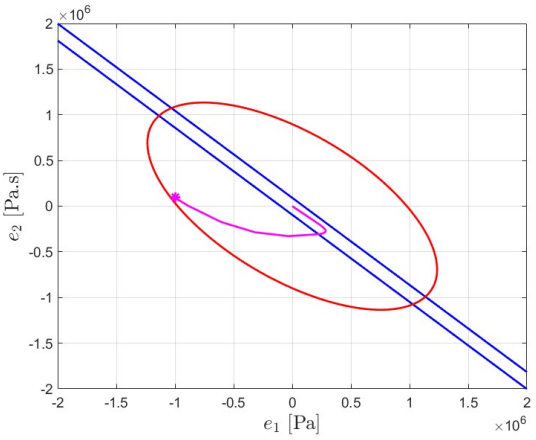

Fig. 8. *Phase plane of e (trajectory in pink), region of linearity (in blue) and estimation of the basin of attraction (in red).*

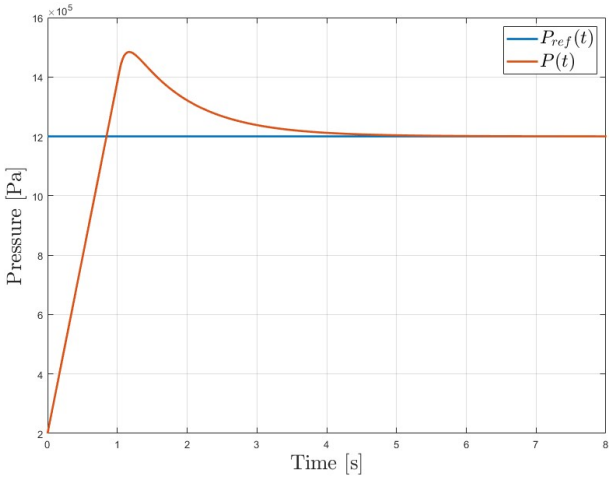

Fig. 9. *Time responses of the output pressure $P(t)$ (in ref) and the reference P_{ref} (in blue).*

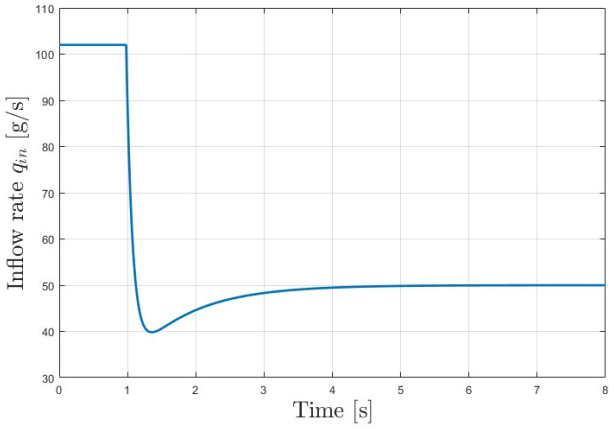

Fig. 10. *Time evolution of the (virtual) control input, that is the inflow rate $q_{int}(t)$.*

$0.013\ mm/g/s$. The LMI (13)-(14) were tested with the objective function trace$(-W)$ so as to maximize the size of the ellipsoidal set ε. The solver solution gives the matrix

$$X = 10^{-11} \begin{bmatrix} 0.1047 & 0.0697 \\ 0.0697 & 0.1241 \end{bmatrix}$$

allows to draw an estimation of the basin of attraction (see Figure 8). A first simulation is performed with an outflow rate $q_{out} = 50\ g/s$ and an initial condition $P(0) = 2\ bar$. The supply pressure, upstream of the actuator, is $50\ bar$ while the desired downstream pressure P_{ref} is $12\ bar$. Figure 8 shows the trajectory of the error coordinates e in the phase plane (the corresponding initial condition is $e(0) = [P(0) - P_{ref}\ ,\ q_{out}/k_2] = -10^6[1\ ,\ 0.09]$), as well as the estimation of the basin of attraction with the above matrix P. Figure 9 shows the time responses of the output pressure $P(t)$ and the its reference. As expected, the error coordinates converge to zero, and thus, the pressure converges to the desired setpoint. It can be seen that for approximately $1\,s$ the system is in saturation mode (see also Figure 10), and being initialized inside the ellipsoid, it ensures the convergence to the origin. Note that the overshoot is a side effect of the integral action with the saturation. An initial condition P_0 closer to the setpoint P_{ref} or a higher maximal rate $q_{\max}$ reduce the overshoot. Future work will be the introduction of an anti-windup control in the design so as to compensate this phenomenon. The virtual control input q_{int}, that is the inflow rate driven by the actuator, is shown in Figure 10. Because the initial pressure is low, the control law asks for maximal rate, limited by $q_{\max} = 102\ g/s$. As expected, at the steady state q_{in} equals q_{out} to balance the output flow and keeps the pressure constant.

B. Experimentation

For the experimental setup, the desired downstream pressure P_{ref} is still $12\ bar$ while tests have been carried for different supply pressures, from $50\ bar$ to $150\ bar$. The proposed control strategy is functional for all tests, here only the case with $P_s = 50\ bar$ is plotted. The outlet flow rate is time-varying with a piecewise constant profile:

$$q_{out}(t) = \begin{cases} 53 & g.s^{-1} \quad 0 \leq t < 5 \\ 74 & g.s^{-1} \quad 5 \leq t < 10 \\ 98 & g.s^{-1} \quad 15 \leq t \end{cases} \tag{16}$$

These changes are due to the application operational requirements downstream the pressure reducer system. The positioning actuator embedded in the testbed is an electromagnetic actuator[2] for which the control system was designed independently and ensures global asymptotic stability and a fast time response (about few milliseconds) [3], [4]. Experimental results are plotted in Figure 11 and 12. It shows that the proposed control system regulates the output pressure P to the desired value, despite the changes of the outlet flow rate (16). The first transient regime is much longer because of the saturation phenomenon. In Figure 12, experimental results are compared to simulation one. The behaviors are fairly similar and it validates the modeling approach. Figure

[2]Also designed by the company CSTM

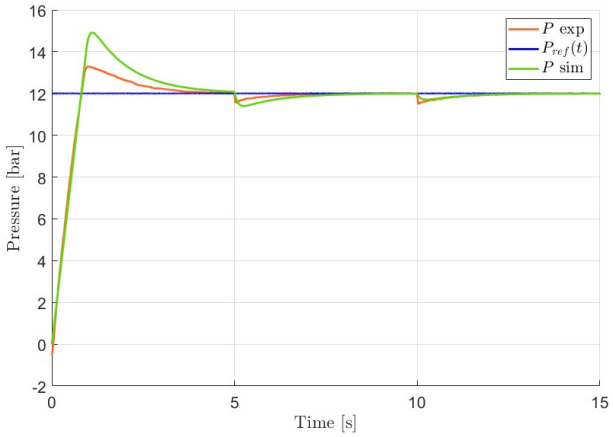

Fig. 11. *Time response of the output pressure $P(t)$: comparison between simulation (in green) and experimentation (in orange) results.*

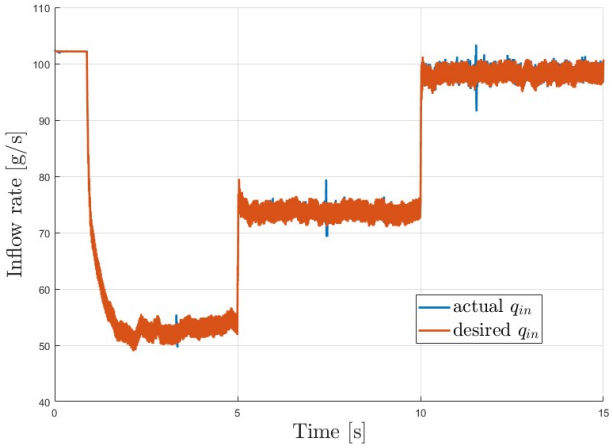

Fig. 12. *Time evolution of the (virtual) control input $q_{int}(t)$: comparison between the desired inflow rate (in orange) and the actual one (in blue).*

12 compares the desired inflow rate $q_{in} = f_{bn}(z_r)$ and the actual one $q_{in} = f_{bn}(z)$. The difference stems from the error dynamic of the actuator. As explained above, this dynamic is very fast, about few milliseconds for a step response, and the curves overlap at the scale of rate dynamic. It can be seen that the control law is able to match each changes of the outflow rate (16) so the pressure reaches an equilibrium point with no steady state error (Figure 11).

V. Conclusion

The physical modeling and the control of a pressure reducing system is proposed in this work. An output feedback with an integral action is developed to ensure local asymptotic stability while taking into account the inflow rate saturation. We also take into account the dynamic of the actuator, integrated in the pressure reducer, that controls the valve position in a decoupled way. The objective was to justify the usual cascade control approach, with an independent design between subsystems while guaranteeing the stability of the overall system. The stability analysis is expressed with LMI conditions that can be easily solved with SDP solvers, and an estimation of the basin of attraction is also provided. The proposed control system was validated through experimental tests on a testbed with dry air. It will be also interested to test others gas like helium or nitrogen.

Future works concern the integration of an anti-windup mechanism in the control scheme and the design of all gains directly from the LMI conditions. From a practical point of view, it would be interesting to address the case when the volume of the downstream chamber is time-varying. Finally, in further experimentation, it would be also interesting to qualify the control law with non-constant reference pressure and pressure tracking trajectory in order to validate the modular use of this equipment.

Acknowledgment

The authors are grateful to Damien De Seze from CNES and François Dugué from CSTM for the grants that have supported this activity.

References

[1] W. Birk and A. Medvedev. Pressure and flow control of a pulverized coal injection vessel. *IEEE Transactions on Control Systems Technology*, 8(6):919–929, 2000.

[2] C. De Persis and C. S. Kallesoe. Pressure regulation in nonlinear hydraulic networks by positive and quantized controls. *IEEE Transactions on Control Systems Technology*, 19(6):1371–1383, 2011.

[3] F. Deschaux, F. Gouaisbaut, and Y. Ariba. Nonlinear control for an uncertain electromagnetic actuator. In *2018 IEEE Conference on Decision and Control (CDC)*, pages 2316–2321, 2018.

[4] F. Deschaux, F. Gouaisbaut, and Y. Ariba. Magnetic force modelling and nonlinear switched control of an electromagnetic actuator. In *2019 IEEE 58th Conference on Decision and Control (CDC)*, pages 1416–1421, 2019.

[5] X. Fan, Y. He, P. Cheng, and M. Fang. Fuzzy-type fast terminal sliding-mode controller for pressure control of pilot solenoid valve in automatic transmission. *IEEE Access*, 7:122342–122353, 2019.

[6] W. Han, L. Xiong, and Z. Yu. Interconnected pressure estimation and double closed-loop cascade control for an integrated electrohydraulic brake system. *IEEE/ASME Transactions on Mechatronics*, 25(5):2460–2471, 2020.

[7] M. Liermann. Pid tuning rule for pressure control applications. *International Journal of Fluid Power*, 14(1):7–15, 2013.

[8] H. Sun, L. Gao, Z. Zhao, and B. Li. Adaptive super-twisting fast nonsingular terminal sliding mode control with eso for high-pressure electro-pneumatic servo valve. *Control Engineering Practice*, 134:105483, 2023.

[9] S. Tarbouriech, G. Garcia, J. Silva, and I. Queinnec. *Stability and Stabilization of Linear Systems with Saturating Actuators*. Springer London, 01 2011.

[10] S. Tarbouriech, C. Prieur, and J.M.G. da Silva. Stability analysis and stabilization of systems presenting nested saturations. *IEEE Transactions on Automatic Control*, 51(8):1364–1371, 2006.

[11] P. Tatiossian, F. Dugué, and F. Roux. Electronic pressure regulator for liquid propulsion rockets. In *Space Propulsion*, Roma, Italy, May 2016.

[12] Q. Wang, H. Yao, Y. He, Y. Yu, and J. Yang. Research on rail pressure control of high-pressure common rail system for marine diesel engine based on controlled object model. *IEEE Access*, 9:125384–125392, 2021.

[13] J. Zhou, O. N. Stamnes, O. M. Aamo, and G.-O. Kaasa. Switched control for pressure regulation and kick attenuation in a managed pressure drilling system. *IEEE Transactions on Control Systems Technology*, 19(2):337–350, 2011.

[14] H. Zhuang, Q. Sun, Z. Chen, and Y. Jiang. Back-stepping sliding mode control for pressure regulation of oxygen mask based on an extended state observer. *Automatica*, 119:109106, 2020.